Forward Equity Risk Premium and Its Economic Implications

July 7, 2022

Abstract

The forward equity risk premium (FERP) is a function of investors' risk aversion and the forward-looking volatility, skewness, and kurtosis of market returns. When estimated from a stochastic volatility model with a mean-reversion variance process, the monthly FERP for the U.S. equity market adequately reflects market conditions and it is always positive. We present evidence that changes in the FERP can predict the growth of real economic activity. The cumulative market excess returns over a period of up to six months are negatively (positively) related to the FERP observed at the beginning of the period in a bear (bull) market. This seesaw effect of FERP on future excess returns has not been discussed before in the asset pricing literature.

Keywords: equity risk premium, return predictability, risk aversion coefficient, real economic activities, stochastic volatility models.

JEL Classification Codes: C53, G12, G14

1 Introduction

The equity risk premium, which measures the excess return compensating investors for taking risk, has been investigated thoroughly over the last few decades. However, a forward-looking method for estimating equity risk premium would add a valuable tool to the economist or the investor looking to manage complex risks in financial markets. Extracting forward-looking information from option prices, Santa-Clara and Yan (2010) derive the equity risk premium as a function of implied volatility and jump intensity. Duan and Zhang (2014) derive the forward equity risk premium (FERP) as a combination of implied volatility, investors' risk aversion and forward-looking physical moments of the returns. Compared to Santa-Clara and Yan (2010), the novel approach in Duan and Zhang (2014) is based on a generic moment expansion of the stochastic discount factor, such that the implied volatility is derived using a model-free option portfolio approach.

Duan and Zhang (2014) compute a FERP that is always positive and it adequately reflects market conditions over their period of study. They deduce the forward-looking market return moments under the physical measure from the nonlinear asymmetric generalized autoregressive conditional heteroskedasticity (NGARCH) model. The forward-looking physical moments of the returns are notoriously difficult to estimate in a model-free manner. However, the FERP estimation framework proposed by Duan and Zhang (2014) is quite general and applicable to other models employed for equity return dynamics.

One drawback mentioned by Duan and Zhang (2014) about their approach to compute the FERP is that the NGARCH model has a high volatility persistence. To address this, we consider the stochastic volatility (SV) model of Heston (1993) to model the behaviour of the volatility of the equity markets. In this model, the volatility is described by a mean-reversion process, avoiding high volatility persistence.[1] Motivated by the results of Santa-Clara and Yan (2010)

[1]In the next sections we highlight that the FERP estimates are sensitive to the model specification used. The

and Maheu et al. (2013), who find that jumps are related to the equity risk premium, we also consider the stochastic volatility model with price jumps, hereafter denoted by SVJ. Using the volatility spread formula developed in Bakshi and Madan (2006), the investors' forward-looking risk aversion coefficient is estimated from the one-month ahead risk-neutral volatility and the one-month forward-looking physical moments of the returns. We use the Chicago Board of Options Exchange (CBOE) Volatility Index (VIX) directly as representative of the one-month risk-neutral volatility. The forward-looking physical moments of the returns are estimated by simulations based on the estimated model parameters, similar to Duan and Zhang (2014). We find that the SVJ model offers the best fit to the data, whilst the NGARCH model can lead to very high values of the forward-looking physical volatility during volatile periods. The forward-looking physical skewness and kurtosis estimated by SV and SVJ always stay in a reasonable range (0 to -2 for skewness and 3 to 6 for kurtosis); however, during 2020, we observe extreme estimates of the forward-looking physical kurtosis of the returns based on the NGARCH model.

We extend the FERP calculated period in Duan and Zhang (2014) to the period January 1999 to October 2020. This period includes major events such as the 2000 dot-com crash, the 9/11 event in 2001, the 2002 WorldCom accounting scandal, the 2007 to 2009 financial crisis, the 2008 to 2014 U.S. quantitative easing, and the 2020 COVID-19 pandemic. Our focus is the one-month FERP and we find that for all models considered, the estimated FERP can adequately reflect market conditions before 2020. However, during the 2020 pandemic, only the FERPs estimated from SV and SVJ, respectively, have a sudden positive jump, whilst the NGARCH model generates a significantly negative FERP in April 2020. Overall, we find that the SV is the only model that produces positive FERP values for our entire research period.

Another main contribution of this paper is the study of the economic implications of the FERP.

high volatility persistence of the NGARCH model is discussed later on in Section 4.

The first question we investigate is whether the FERP can predict real economic activities (REA). Economic recessions tend to follow financial market crashes (Gourinchas and Obstfeld, 2012 and Faccini et al., 2019). The FERP reflects the investors' perceptions about the future state of the economy and thus it can be informative about future REA growth. We find that the change in FERP, estimated by the SV and SVJ models, has significant power in predicting all selected REA growth indicators both in- and out-of-sample, whilst the NGARCH FERP is a significant predictor only for some of the activities.

The second question we investigate is whether the FERP can predict future cumulative market excess returns. Duan and Zhang (2014) find a negative relationship between the change in FERP and future market excess returns. However, the negative relationship between FERP and market excess return is not consistent with the intuition of a market risk premium. Investors will look to be compensated for taking risk and we explore the association between cumulative market excess returns and the value of the FERP at the beginning of the period using quantile regressions. We find that the FERP has predictive power for the market excess returns especially in the lower and upper quantiles. The cumulative market excess returns are predicted to increase (decrease) with FERP when the market is bullish (bearish), indicating that investors receive compensation for taking forward risk in a bull market. This seesaw effect of FERP on future returns has not been captured in the previous literature on asset pricing.

The rest of the paper is organized as follows: Section 2 introduces the theoretical framework of FERP. Section 3 presents the FERP estimation methods. Section 4 describes the estimated forward-looking physical moments of the returns, the investors' risk aversion coefficient and the FERP. The prediction of real economic activities and market excess returns with FERP are discussed and presented in Sections 5 and 6, respectively. The last section summarizes our conclusions.

2 The Theory of Forward Equity Risk Premium

In the following, S_t denotes the market portfolio's value at time t, and the continuously compounded return over the period t to $t+\tau$ is $R_t(\tau) = \ln(S_{t+\tau}/S_t)$. To describe the distribution of the market portfolio's returns, the mean, standard deviation, skewness and kurtosis of the returns, $R_t(\tau)$, under the physical probability measure $\mathbb{P}$, over the time period t to $t+\tau$, are denoted as $\mu_t^{\mathbb{P}}(\tau)$, $\sigma_t^{\mathbb{P}}(\tau)$, $Skew_t^{\mathbb{P}}(\tau)$ and $Kurt_t^{\mathbb{P}}(\tau)$, respectively. The risk-neutral equivalents of these measures, which characterize the returns' distribution implied by option prices data, are denoted by $\mu_t^{\mathbb{Q}}(\tau)$, $\sigma_t^{\mathbb{Q}}(\tau)$, $Skew_t^{\mathbb{Q}}(\tau)$ and $Kurt_t^{\mathbb{Q}}(\tau)$, respectively.

Let $r_t(\tau)$ and $\delta_t(\tau)$ represent the continuously compounded risk-free interest rate and the dividend yield of the market portfolio S, respectively, over the time period t to $t+\tau$. The risk-free rate can be expressed using the risk-neutral moments as given in the following approximate relationship:[2]

$$r_t(\tau) \approx \delta_t(\tau) + \mu_t^{\mathbb{Q}}(\tau) + \frac{1}{2}\sigma_t^{\mathbb{Q}}(\tau)^2 + \frac{1}{6}\sigma_t^{\mathbb{Q}}(\tau)^3 Skew_t^{\mathbb{Q}}(\tau) + \frac{1}{24}\sigma_t^{\mathbb{Q}}(\tau)^4 \left[Kurt_t^{\mathbb{Q}}(\tau) - 3\right]. \quad (1)$$

The above relationship does not depend on the form of the stochastic discount factor. However, the form of the stochastic discount factor is required when expressing the risk-free rate using the moments of the physical returns. Assuming that the representative agents' preferences are described by a power utility function (see Duan and Zhang, 2014 and Faccini et al., 2019), the τ-period stochastic discount factor can be expressed as $e^{\gamma_t(\tau)R_t(\tau)}$, where $\gamma_t(\tau)$ is the risk aversion coefficient and the moment generating function of $R_t(\tau)$ should exist under both probability measures $\mathbb{P}$ and $\mathbb{Q}$. The risk aversion coefficient $\gamma_t(\tau)$ can be extracted from the following expression for the volatility

[2]See Appendix A in Duan and Zhang (2014) for the derivation of this relationship.

spread (Bakshi and Madan, 2006):

$$\frac{\sigma_t^{\mathbb{Q}}(\tau)^2 - \sigma_t^{\mathbb{P}}(\tau)^2}{\sigma_t^{\mathbb{P}}(\tau)^2} \approx -\gamma_t(\tau)\sigma_t^{\mathbb{P}}(\tau)Skew_t^{\mathbb{P}}(\tau) + \frac{\gamma_t(\tau)^2}{2}\sigma_t^{\mathbb{P}}(\tau)^2\left[Kurt_t^{\mathbb{P}}(\tau) - 3\right]. \tag{2}$$

Based on the power utility assumption, $\mu_t^{\mathbb{Q}}(\tau)$, $\sigma_t^{\mathbb{Q}}(\tau)$, $Skew_t^{\mathbb{Q}}(\tau)$ and $Kurt_t^{\mathbb{Q}}(\tau)$ can be expressed in terms of the moments of the physical returns. By substituting these expressions into Equation (1), the τ-period equity risk premium at time t can be derived as a function of the investors' risk aversion, physical return variance, skewness, and kurtosis:[3]

$$\begin{aligned}\mu_t^{\mathbb{P}}(\tau) + \delta_t(\tau) - r_t(\tau) \approx \left[\gamma_t(\tau) - \frac{1}{2}\right]\sigma_t^{\mathbb{P}}(\tau)^2 - \frac{3\gamma_t(\tau)^2 - 3\gamma_t(\tau) + 1}{6}\sigma_t^{\mathbb{P}}(\tau)^3 Skew_t^{\mathbb{P}}(\tau) \\ + \frac{4\gamma_t(\tau)^3 - 6\gamma_t(\tau)^2 + 4\gamma_t(\tau) - 1}{24}\sigma_t^{\mathbb{P}}(\tau)^4\left[Kurt_t^{\mathbb{P}}(\tau) - 3\right].\end{aligned} \tag{3}$$

The forward equity risk premium for the period t to $t+\tau$ can be calculated from Equation (3) if the forward-looking risk aversion coefficient and the physical moments of the returns for the same horizon are estimated at time t. The estimation of these forward-looking parameters are described in the next section. If the asset's returns follow a normal distribution, that is, $Skew_t^{\mathbb{P}}(\tau) = 0$ and $Kurt_t^{\mathbb{P}}(\tau) = 3$, then the equity risk premium is equal to $\left[\gamma_t(\tau) - \frac{1}{2}\right]\sigma_t^{\mathbb{P}}(\tau)^2$. However, the presence of physical skewness and excess kurtosis will affect the estimates of the equity risk premium. In the second term on the right hand side of Equation (3), $3\gamma_t(\tau)^2 - 3\gamma_t(\tau) + 1$ is always positive, implying that a negative (positive) skewness drives up (down) the equity risk premium. In the third term on the right hand side of Equation (3), $4\gamma_t(\tau)^3 - 6\gamma_t(\tau)^2 + 4\gamma_t(\tau) - 1$ is positive when $\gamma_t(\tau) > \frac{1}{2}$. This indicates that the fat tails of the asset's returns can increase the equity risk premium when the investors' risk aversion coefficient is greater than $\frac{1}{2}$.

[3]The proof can be found in Appendix B in Duan and Zhang (2014).

3 Estimation of the Forward-Looking Risk Aversion and the Physical Moments of the Returns

To estimate the FERP, we first need to obtain the estimates of the parameters in (3). As in Bakshi and Madan (2006) and Duan and Zhang (2014), we estimate the τ-period risk aversion coefficient, $\gamma_t(\tau)$, from Equation (2) which describes the volatility spread. Specifically, the generalized method of moments (GMM) is applied with the following orthogonality condition:

$$\mathrm{E}\left\{ \frac{\sigma_t^{\mathbb{Q}}(\tau)^2 - \sigma_t^{\mathbb{P}}(\tau)^2}{\sigma_t^{\mathbb{P}}(\tau)^2} + \hat{\gamma}(\tau)\sigma_t^{\mathbb{P}}(\tau)Skew_t^{\mathbb{P}}(\tau) - \frac{\hat{\gamma}(\tau)^2}{2}\sigma_t^{\mathbb{P}}(\tau)^2\left[Kurt_t^{\mathbb{P}}(\tau) - 3\right] \middle| I_t \right\} = 0, \qquad (4)$$

where I_t denotes the information set at time t, including the time series of risk-neutral volatility and three time series for the higher moments of the physical returns. As in Duan and Zhang (2014) the τ-period risk aversion coefficient in Equation (4) is denoted by $\hat{\gamma}(\tau)$ without the subscript t, because the estimation will lead to an overall estimate of the τ-period risk aversion.

To estimate the risk aversion coefficient, the time series of the risk-neutral volatility and the moments of the physical returns are required. In this paper, we focus on the one-month FERP, and the CBOE VIX is used as the proxy for the risk-neutral volatility, $\sigma_t^{\mathbb{Q}}(\tau)$. The VIX index is computed from a panel of S&P 500 index options and represents the risk-neutral expectation of the S&P 500 index volatility over the next month. This has been used as the option-implied risk-neutral volatility in many studies, such as Yang and Zhou (2017), Doshi et al. (2018) and Bae and Elkamhi (2021).

We estimate the forward-looking physical moments of the returns under the SV model proposed by Heston (1993). Duan and Zhang (2014) adopt the nonlinear asymmetric generalized autoregressive conditional heteroskedasticity model of Engle and Ng (1993), denoted by NGARCH, to estimate the moments of the physical returns. As stated in Duan and Zhang (2014), the specification of

the NGARCH model leads to a very high volatility persistence; thus, the simulation noise cannot be attenuated quickly and it can lead to large swings in the simulated skewness and kurtosis. By contrast, the volatility process of the SV model is described by a mean-reversion process, which can avoid high persistence in the volatility. To investigate the effect of jumps on estimating FERP, we also consider the SVJ model, which is the SV model with added Poisson jumps in the return process.

The dynamic of the daily asset returns implied by the SVJ model under the physical probability measure $\mathbb{P}$ is assumed to follow the process below:

$$\begin{aligned} \ln\frac{S_{t+1}}{S_t} &= \mu + \sqrt{V_t}\epsilon^R_{t+1} + J^R_{t+1}, \\ V_{t+1} &= V_t + \kappa(\theta - V_t) + \sigma_V\sqrt{V_t}\epsilon^V_{t+1}, \end{aligned} \tag{5}$$

where ϵ^R_{t+1} and ϵ^V_{t+1} follow the standard normal distribution and are correlated with correlation coefficient ρ, ϵ^R_{t+1} is the residual for returns; μ is the daily mean return and V_t denotes the instantaneous variance at t. The variance is a mean-reversion process, where κ represents the reversion speed; θ is the long-run mean of the variance and σ_V denotes the volatility of volatility. The jump process is defined by $J^R_{t+1} = \xi^R_{t+1}N^R_{t+1}$, where $\{N^R_{t+1}\}_{t\geq 0}$ is the Poisson process with intensity λ and $\xi^R_{t+1} \sim \mathbb{N}(\mu_J, \sigma^2_J)$ represents the size of the jump.[4] The SV model is obtained by setting $\lambda = 0$.

The parameters of the SV and SVJ models are estimated using Markov-chain Monte Carlo (MCMC) methods, a more detailed description is provided in the Appendix. As SVJ nests SV, in the following we only present the estimation method for the SVJ model. Let $\Theta = \{\mu, \kappa, \theta, \sigma_v, \rho, \lambda, \mu_J, \sigma_J\}$ denote the parameter vector of the SVJ model and $p(\Theta)$ be the priors of Θ. Given the stock prices $S = \{S_t\}_{t\in\{0,\ldots,T\}}$, the variance series $V = \{V_t\}_{t\in\{0,\ldots,T\}}$, and the jumps times/sizes $J = \{J_t\}_{t\in\{0,\ldots,T\}}$, the posterior of parameters and latent variables can be decomposed into the product

[4] $\mathbb{N}$ denotes the Normal distribution.

of individual conditionals as follows:

$$p(\Theta, V, J|S) \propto p(S, V, J, \Theta) = p(S, V|J, \Theta)p(J|\Theta)p(\Theta). \tag{6}$$

The priors and posteriors of each parameter and latent variables are documented in the Appendix. The MCMC estimation process has 100,000 iterations in total, and the first 50,000 draws are discarded as "burn-in". The posterior means are taken as the estimated parameter values. After obtaining the parameter estimates, a simulation method is applied to estimate the forward-looking physical moments of the returns. We simulate the model based on Equation (5) to obtain the asset's cumulative returns from $t+1$ to $t+\tau$ based on the estimated parameters and variance at time t. The simulation setup has $N^* = 300,000$ runs, and the forward-looking physical moments of the returns are computed using their sample equivalents. Algorithm 1 provides a detailed description of the method.

Algorithm 1: Estimation of the Forward-Looking Physical Moments of the Returns

Input: stock prices before time t, the length of the forward-looking period τ and the number of simulation draws N^*.
Output: $\sigma_t^{\mathbb{P}}(\tau)$, $Skew_t^{\mathbb{P}}(\tau)$ and $Kurt_t^{\mathbb{P}}(\tau)$.
Model Estimation: estimate the model parameters based on the stock prices before t using MCMC and obtain the estimated parameters $\widehat{\Theta}$ as well as the estimated variance at time t, $\widehat{V}_t$.
Initialization: $\iota = 1$;
Simulation: while $\iota \leq N^*$ **do**
  simulate the daily returns from $t+1$ to $t+\tau$ with $\widehat{\Theta}$ and $\widehat{V}_t$ using Equation (5) and obtain the simulated τ-period return $R_t^{(\iota)}(\tau)$.
Output Computation: Compute $\sigma_t^{\mathbb{P}}(\tau)$, $Skew_t^{\mathbb{P}}(\tau)$ and $Kurt_t^{\mathbb{P}}(\tau)$ as the volatility, skewness and kurtosis of all the simulated τ-period returns, $\tilde{R}_t$, where $\tilde{R}_t = \left\{R_t^{(\iota)}(\tau)\right\}_{\iota=1}^{N^*}$.
return: $\sigma_t^{\mathbb{P}}(\tau)$, $Skew_t^{\mathbb{P}}(\tau)$ and $Kurt_t^{\mathbb{P}}(\tau)$.

We compare our results with those obtained with the NGARCH model following Duan and Zhang (2014). The NGARCH model is estimated using the quasi-maximum likelihood estimation method, as in Duan and Zhang (2014), and the forward-looking physical variance of the returns is

calculated analytically,[5] with the skewness and kurtosis computed with a parametric bootstrapping method.[6]

4 Empirical Analysis on the Forward Equity Risk Premium

4.1 Data and Estimation

The data consists of daily S&P 500 index closing prices, ranging from January 3, 1989 to September 30, 2020, and the CBOE VIX on the last trading day of each month over the period January 1994 to September 2020. The S&P 500 index prices are obtained from Bloomberg, and the VIX data is downloaded from the CBOE website. We use an estimation window of five years to estimate the forward-looking moments of returns, which leads to the estimated forward-looking moments of the returns after January 1994. The FERP starting with January 1999 is then estimated with five-year forward-looking moments of returns and VIX.

We estimate the models monthly using the S&P 500 index daily closing prices over the five years before the first trading day of each month during the period from January 1994 to October 2020 (322 months in total). The estimated parameters are then used to approximate the forward-looking physical moments of the one-month returns (corresponding to 22 trading days).[7]

After the model parameters are estimated in each estimation window, we obtain 322 sets of return residuals for each model. For a goodness-of-fit comparative analysis, we apply the Kolmogorov-Smirnov (KS) test with the improved adjustment of Abadie (2002) to the return residuals. The null

[5]The estimated moments are expected to converge to the analytically computed equivalents. The expected values of the realized moments for SV and SVJ can also be obtained analytically when the market is continuously monitored (Amaya et al., 2015). However, as daily data is used in this study, the continuously monitored values are not entirely appropriate.

[6]Our simulation-based method is in the spirit of the parametric bootstrapping method in Duan and Zhang (2014) with the main difference being the choice of random variables. Duan and Zhang (2014) resample the random variables from the estimated residuals, while we generate them directly from the standard normal distribution they follow.

[7]The VIX is constructed to be a general measure of the market's estimate of the average S&P 500 volatility over the subsequent 22 trading days (see Connolly et al., 2005 and Bekaert and Hoerova, 2014).

hypothesis of the test is that the residuals follow the standard normal distribution. To compare the performance of the models, in Table 1 we report the ratio of KS test rejections for all models at different significance levels. The test is rejected twice at 1% level for the return residuals estimated by the NGARCH model, whilst the return residuals estimated by SV and SVJ pass the KS test in all cases. We obtain that, for NGARCH, for 225 (134) out of 322 sets of return residuals the KS test rejects normality at 10% (5%) significance level, whilst the rejection rates for SV and SVJ are much lower. The results suggest that the SV and SVJ models provide a better fit to the data than the NGARCH model.

To further compare the residuals generated by different models, in Figure 1 we present the annual boxplots of the return residuals for all three models. We reconstitute the twelve sets of return residuals obtained for each year (nine sets of return residuals in 2020) into one array to obtain the corresponding boxplot of residuals for that year. The return residuals obtained from the NGARCH model contain many extreme negative values; by contrast, the values of the return residuals are all smaller than 5 (except for the SV model in 1994) for the SV and SVJ models. Compared with SV, the return residuals implied by the SVJ model have fewer extreme values as most of these can be explained by jumps.

Table 1: KS Abadie Test Rejection Ratios

	SV	SVJ	NGARCH
1%	0% (0)	0% (0)	0.62% (2)
5%	2.18% (7)	0.31% (1)	41.74% (134)
10%	28.97% (93)	9.97% (32)	70.09% (225)

Note: This table reports the ratio and corresponding number of occurrences (presented in parentheses) of rejecting the null hypothesis of the KS test at different significance levels (1%, 5% and 10%). The KS test p-values are adjusted with Abadie's method. The models are estimated using the S&P 500 index daily closing prices over the five years before the first trading day of each month during the period from January 1994 to October 2020 (322 months in total).

Figure 1: Annual Boxplots of the Residuals.

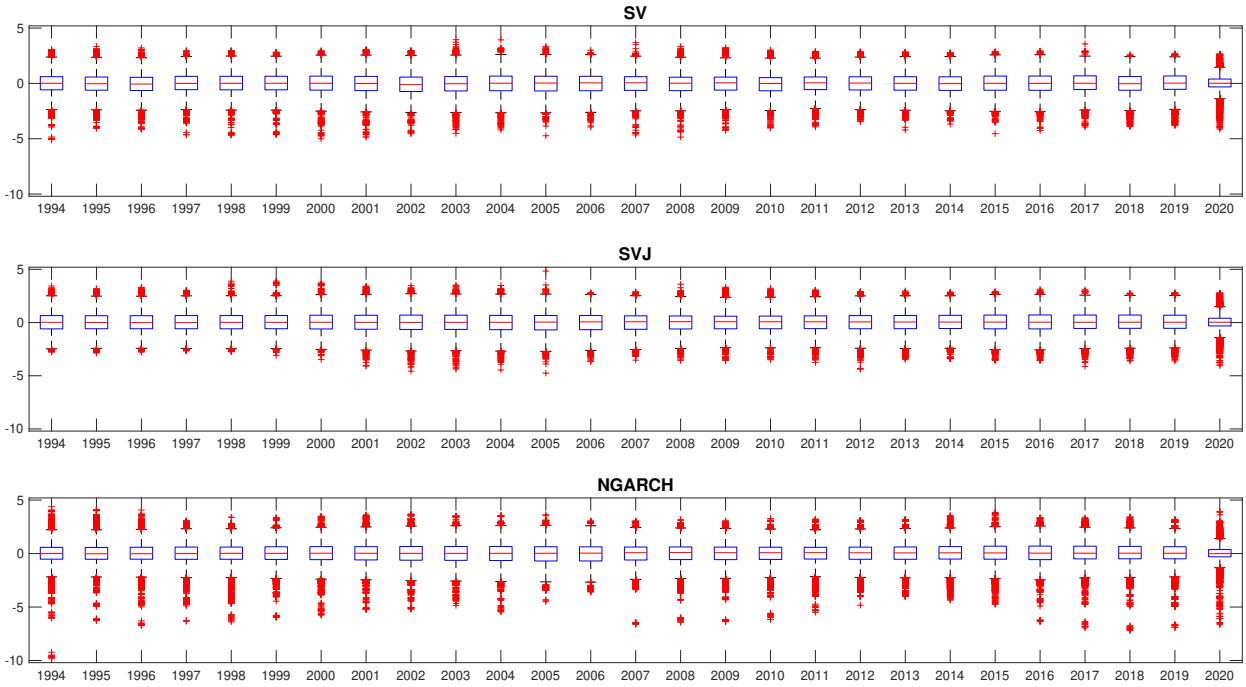

Note: This figure presents the boxplots of the return residuals for SV, SVJ and NGARCH annually from 1994 to 2020. In each box, the central mark represents the median, and the bottom and top edges of the box mark the 25th and 75th percentiles, respectively. The whiskers extend to the most extreme data points not considered outliers, and the outliers are plotted individually using the '+' marker symbol.

4.2 Forward-Looking Physical Moments of the Returns

Figure 2 plots the time series of the one-month forward-looking physical return from January 1994 to October 2020 volatility estimated with the SV, SVJ and NGARCH models. The forward-looking volatilities obtained with these three models display similar features. However, the NGARCH model is likely to generate higher volatility estimates than SV and SVJ when the market is turbulent; by contrast, SVJ leads to lower forward-looking volatility during volatile periods, because the returns can partially be explained by jumps. The average values of the volatility spread, which is calculated as the difference between VIX and the one-month forward-looking physical volatility, are 4.04% for SV, 3.70% for SVJ and 2.99% for NGARCH. These values are in line with previous studies, e.g., Bakshi and Madan (2006), Bali and Hovakimian (2009) and Duan and Zhang (2014).

Figure 2: The One-Month Forward-Looking Physical Volatility.

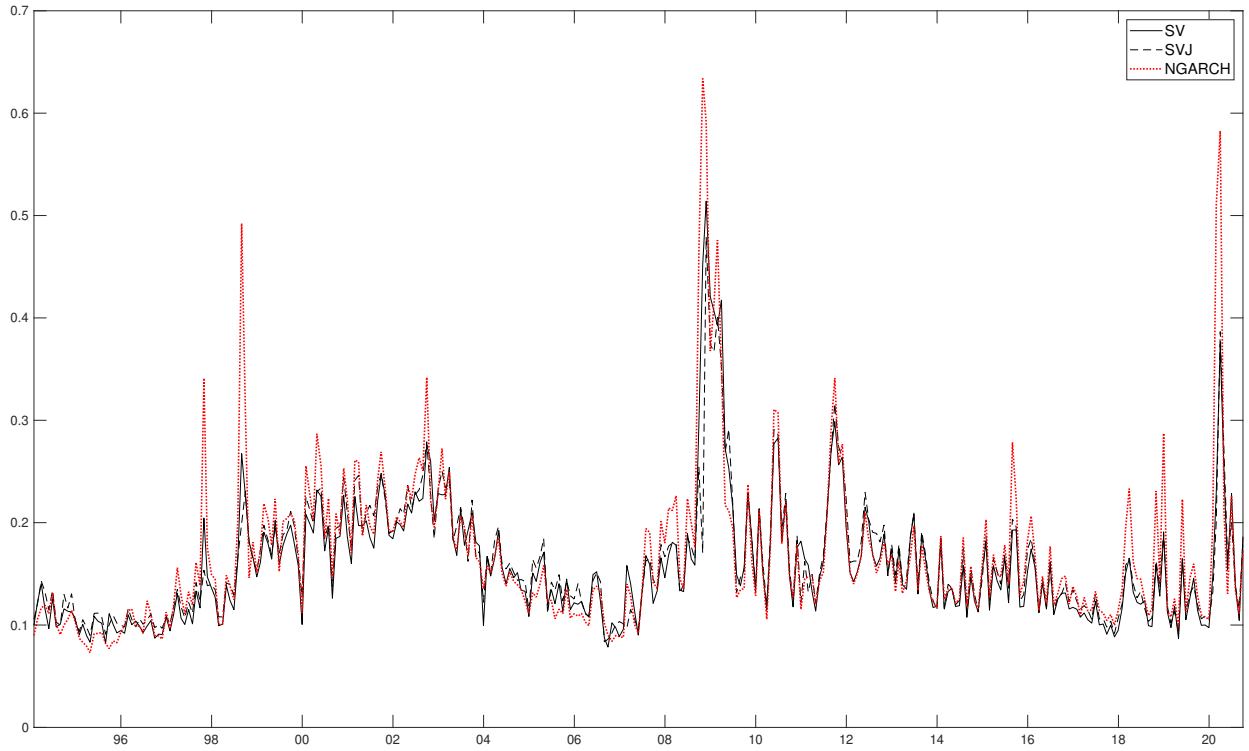

Note: This figure plots the time series of the one-month forward-looking annualized volatility estimates obtained with the SV, SVJ and NGARCH models from January 1994 to October 2020.

Figure 3 plots the time series of the one-month forward-looking physical skewness and kurtosis of the returns. The one-month forward-looking returns are negatively skewed and leptokurtic. The first and third panels present the results for SV and SVJ. These two models lead to very similar results with negative skewness greater than -2 and kurtosis ranging from 3 to 6. However, the NGARCH model leads to extremely large estimates for the forward-looking kurtosis in 2020, as demonstrated in the fourth panel of Figure 3. The reason for this is that the simulated returns generated with NGARCH tend to have very large negative values during 2020, resulting in extreme values for the estimated forward-looking kurtosis. Duan and Zhang (2014) state that the specification of the NGRACH model results in a very high volatility persistence. This leads to large swings in the simulated skewness and kurtosis.[8]

[8]Our estimated forward-looking skewness and kurtosis for the NGARCH models are almost the same as those reported in Duan and Zhang (2014) during their sample period. A comparison can be found in the online Supplementary

Figure 3: The One-Month Forward-Looking Physical Skewness and Kurtosis.

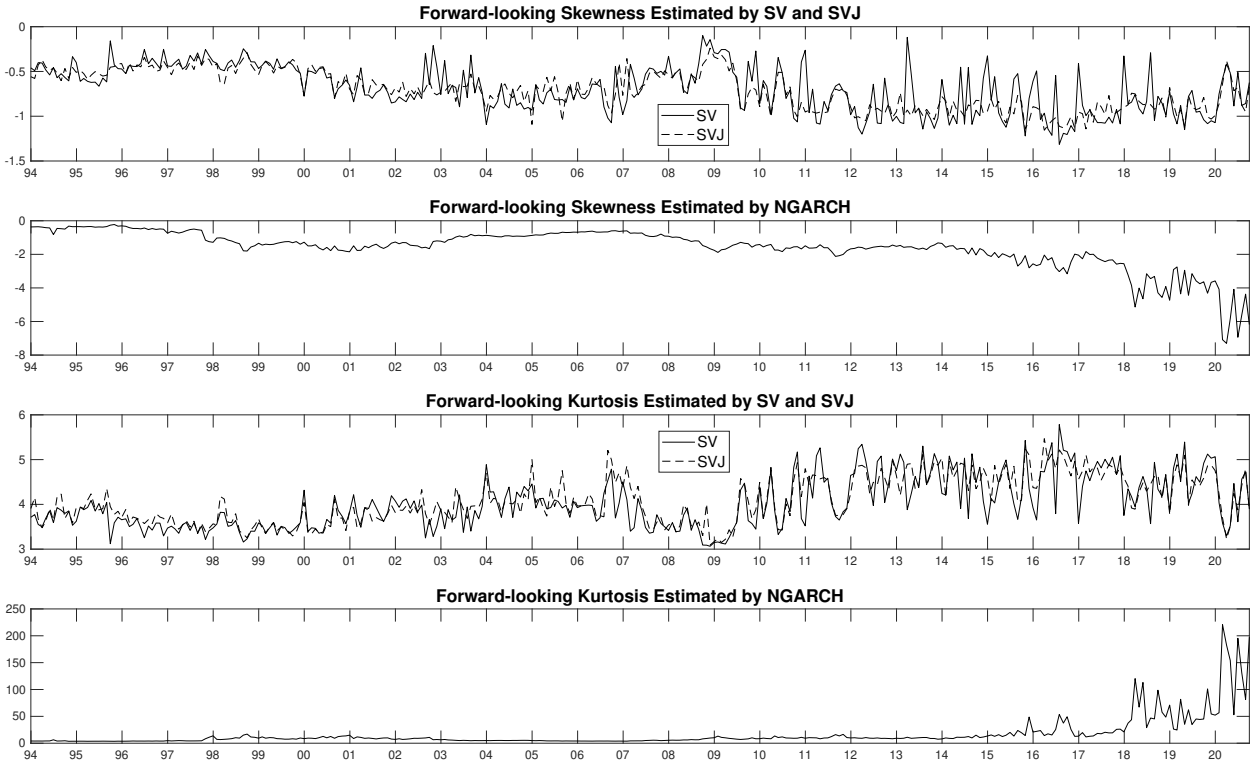

Note: The first and third panels plot the time series of the one-month forward-looking physical skewness and kurtosis of the returns from January 1994 to October 2020 estimated with SV and SVJ. The second and fourth panels plot the one-month forward-looking skewness and kurtosis from January 1994 to October 2020 estimated with NGARCH.

4.3 Forward Equity Risk Premium

The previous section provides us with the forward-looking physical moments of the returns for the models considered. The next step is to estimate the risk aversion coefficient based on these physical moments of the returns and the VIX index. Following Duan and Zhang (2014), $\gamma_t(\tau)$ is estimated with five-year (60-month) monthly data before and including time t. Since the series of the forward-looking physical moments of the returns starts from January 1994, we can estimate the investors' risk aversion starting with January 1999. Following Bakshi and Madan (2006), we use three sets of instruments in the GMM estimation. Specifically: (1) a constant and $\sigma^{\mathbb{Q}}_{t-1}(\tau)^2$; (2) a constant, $\sigma^{\mathbb{Q}}_{t-1}(\tau)^2$ and $\sigma^{\mathbb{Q}}_{t-2}(\tau)^2$; and (3) a constant, $\sigma^{\mathbb{Q}}_{t-1}(\tau)^2$, $\sigma^{\mathbb{Q}}_{t-2}(\tau)^2$ and $\sigma^{\mathbb{Q}}_{t-3}(\tau)^2$. Consistent with Duan

Appendix.

and Zhang (2014), we find that the estimates obtained with these three sets of instruments are very close. In the following, we use the results obtained from the third set of instruments.

Figure 4: Estimated Risk Aversion Coefficient

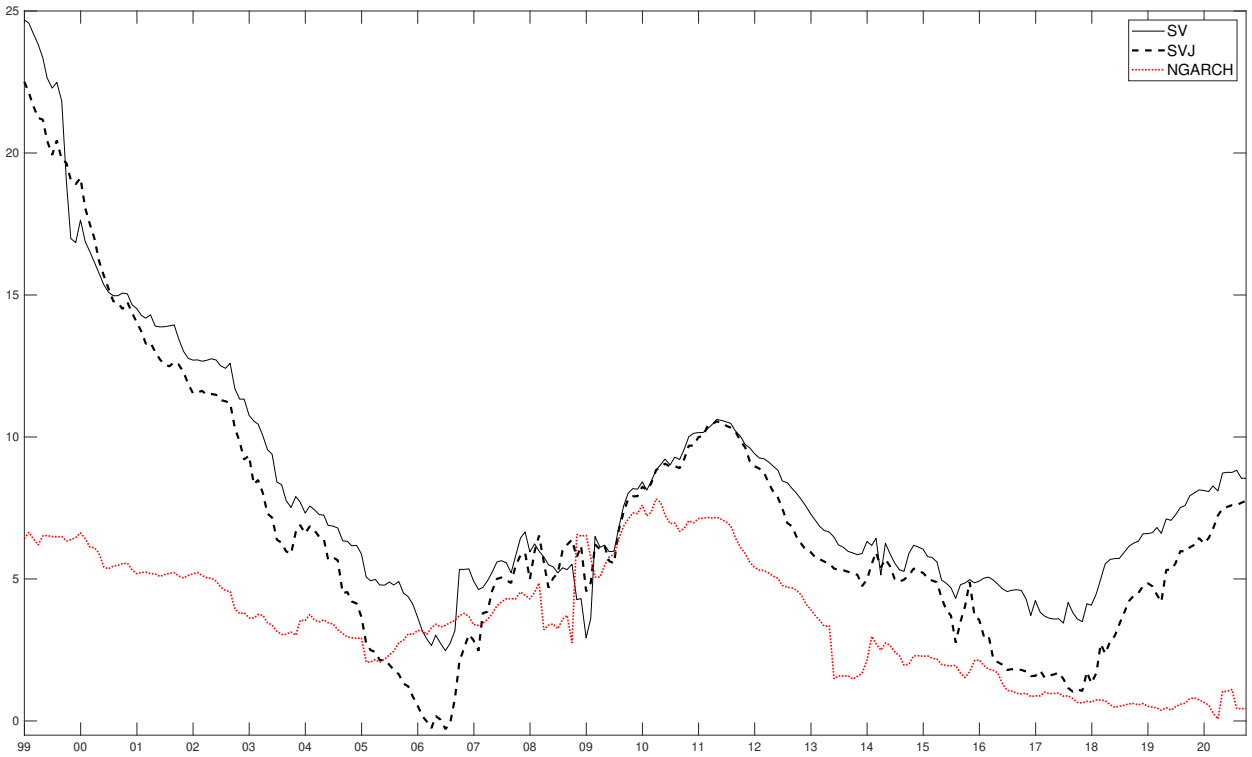

Note: This figure plots the estimated risk aversion coefficient from January 1999 to October 2020 for SV, SVJ and NGARCH.

Figure 4 plots the time-varying monthly risk aversion coefficient from January 1999 to October 2020. The three time series of the risk aversion coefficient are estimated using the one-month forward-looking physical moments of the returns obtained with the SV, SVJ and NGARCH models. The risk aversion estimates for all models range from just below zero to almost 25. This is generally in line with previous studies as follows: 12.70 for the whole sample in Aït-Sahalia and Lo (2000); 2.26 to 12.55 in Rosenberg and Engle (2002); 12.71 to 17.33 in Bakshi and Madan (2006); 1.30 to 6.01 in Duan and Zhang (2014); and 2.27 to 9.55 in Faccini et al. (2019). Compared with the NGARCH model, the SV and SVJ models tend to generate higher risk aversion estimates, especially before 2004. According to the orthogonality condition (4), a higher volatility spread

can lead to a greater risk aversion estimate.[9] The higher risk aversion estimates before 2004 stem from the apparent differences between VIX and the forward-looking physical volatility estimated by the three models between 1996 and 1999, as 60-month data is used in the estimation. The comparison between VIX and estimated forward-looking physical volatility can be found in Figure A3 in the Supplementary Appendix. The risk aversion estimates obtained with SV and SVJ are much greater than those obtained with NGARCH, and this is because the differences between VIX and the forward-looking volatility estimated by NGARCH are relatively low. The larger volatility spread of SV and SVJ results in a higher and declining risk aversion estimates from 1999 to 2004 as five-year data are used in the estimation process. As discussed in Section 2, if the investor's risk aversion is lower than $\frac{1}{2}$, the FERP can be negative. The risk aversion implied by SV is always greater than $\frac{1}{2}$. The risk aversion estimated by SVJ is lower than $\frac{1}{2}$ during the period February 2006 to August 2006; the NGARCH risk aversion is always positive, but we find 12 estimates lower than $\frac{1}{2}$ after June 2018.[10]

The one-month ahead FERP is computed monthly by substituting the investor's risk aversion and the moments of the forward-looking physical returns in Equation (3). The estimated FERP series are presented in Figure 5. All models produce high FERP during the high volatility periods (e.g. the dot-com crash from March 2000 to October 2002; the global financial crisis of 2008 and the European credit crisis that started at the end of 2009). However, during the 2020 COVID-19 pandemic, only the FERP estimates obtained with SV and SVJ respond to the pandemic with a sudden positive spike in April 2020. The SV and SVJ FERPs are consistent with the common belief that investors require a bigger compensation for taking on more risk, and thus the FERP should be high when the market is bearish. By contrast, the NGARCH FERP exhibits a sharp

[9] A similar discussion can be found in Drechsler (2013).

[10] The risk aversion implied by SVJ is negative in March, April, July and August 2006, implying that the representative agent shows a risk-loving behavior over those four months. Faccini et al. (2019) also document negative risk aversion values.

Figure 5: Forward Equity Risk Premium

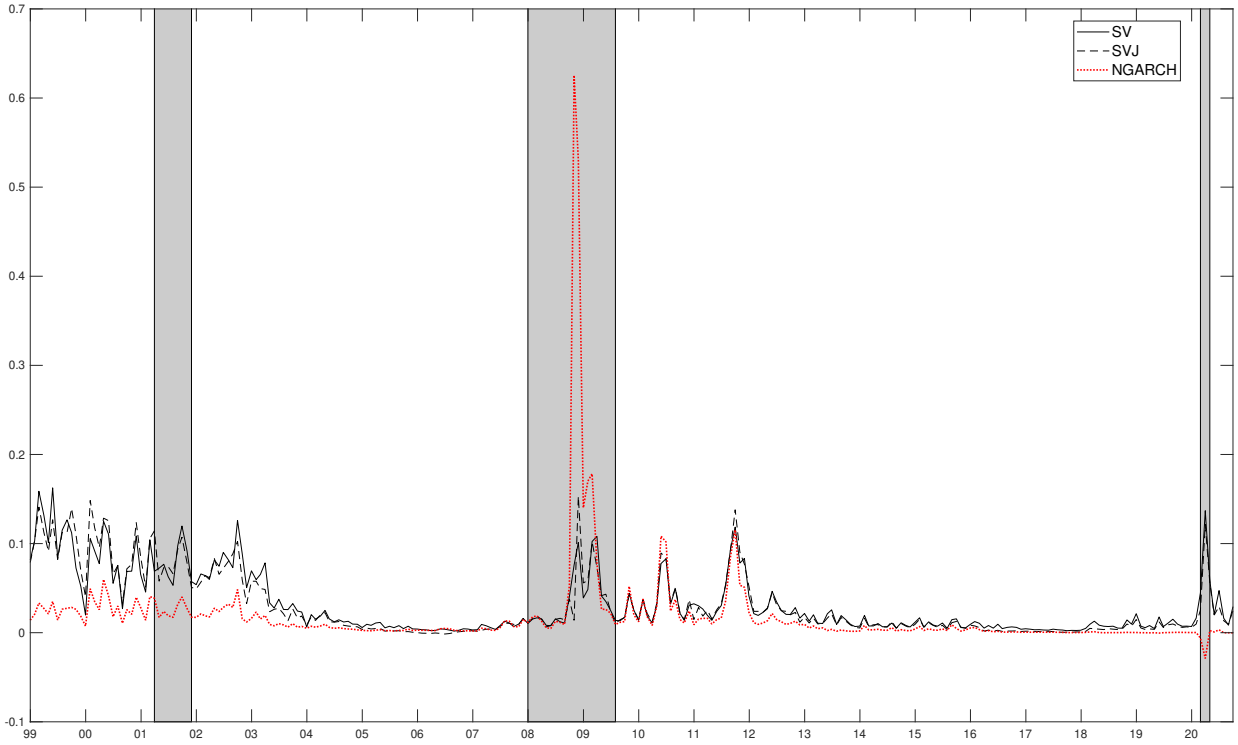

Note: This figure presents the monthly one-month ahead forward equity risk premium from January 1999 to October 2020, estimated using the SV, SVJ and NGARCH models. The grey areas indicate the National Bureau of Economic Research recession periods.

negative spike during 2020. The reason for the negative FERP under the NGARCH model is that the risk aversion coefficient was estimated to be below $\frac{1}{2}$ along with high forward-looking physical volatility and kurtosis of the returns.

The summary statistics of the FERP are reported in Panel A of Table 2. The average values of the FERP are just over 0.03 for SV and SVJ and about 0.02 for the NGARCH model. It is worth noting that the SV model is the only model which produces positive FERP for the entire research period, with a minimum value of around 0.0018. The SVJ has seven negative FERP estimates over the period February 2006 to August 2006, when the risk aversion is below $\frac{1}{2}$. Previewing the quantile regression results in Section 6, we find that the SVJ FERP is positively linked to the future cumulative market excess returns in a bull market. The NGARCH model also reveals 11

negative FERP after June 2018 and reaches its lowest point, about -0.0288, in April 2020. This is counterintuitive as a high FERP is expected during the COVID-19 recession. Whilst, the skewness and kurtosis of the FERP obtained with the SV and SVJ models are quite similar and small. The values of the skewness and kurtosis of NGARCH FERP are more extreme.

Table 2: Summary Statistics and Correlation Matrix of the Forward Equity Risk Premium

	SV	SVJ	NGARCH
Panel A. Summary Statistics			
Mean	3.1630	3.0154	1.8491
Std	3.4933	3.6417	5.4751
Min	0.1771	-0.1474	-2.8837
Max	16.2508	15.3213	62.5693
Skew	1.5212	1.5174	8.6375
Kurt	4.5088	4.3482	88.0163
Panel B. Correlation Matrix			
SV	1.0000		
SVJ	0.8242	1.0000	
NGARCH	0.2614	0.0954	1.0000

Note: This table shows the summary statistics (in Panel A, expressed in percentage) and the correlation matrix (in Panel B) of the one-month forward equity risk premium estimated by SV, SVJ and NGARCH. The results reported are calculated based on monthly values from January 1999 to October 2020.

5 Forecasting the U.S. Real Economic Activity

Growth in the real economic activity can have multiple impacts. Based on REA growth forecasts, the national monetary and fiscal policies, the development plans of the firms, as well as investors' investment strategies need to be adjusted. The link between financial markets and the REA growth has been extensively studied. Stock and Watson (2003) predict REA growth using several financial factors. Gourinchas and Obstfeld (2012) document how the 2008 financial crisis lead to economic recession, whilst Faccini et al. (2019) extract the risk aversion from S&P 500 index options and find that the investors' risk aversion is negatively linked to future REA growth. This section explores the impact of FERP, which contains forward-looking information of the S&P 500 index under both the physical and risk-neutral probability measures, on future cumulative REA growth.

We consider six indicators of REA in the U.S. economy from January 1999 to October 2020.

These proxies are: the logarithmic growth rate (LGR) of industrial production (IP), the LGR of nonfarm payroll employment (NFP), the LGR of retail sales (RS), the LGR of housing starts (HS), the Chicago Fed National Activity Index (CFNAI), and the Aruoba–Diebold–Scotti (Aruoba et al., 2009) business conditions index (ADS). IP measures the industries output, NFP is the number of employees in the nonfarm sectors, RS is the real retail sales including food services sales, HS measures the total newly started privately-owned housing units, CFNAI is constructed based on the methodology described in Stock and Watson (1999), and the ADS is computed according to six economic indicators with different frequencies.[11] The monthly data of IP, NFP, RS, HS and CFNAI are obtained from the Federal Reserve Economic Data (FRED) database, the daily ADS data is downloaded from the Philadelphia Fed webpage, and we take its monthly average as the observation for each month. Table 3 presents the summary statistics and the correlation matrix for the six real economic activity proxies. IP, NFP, CFNAI and ADS are highly correlated, while the correlations between HS and the other REA proxies are much smaller.

Following Faccini et al. (2019), we also consider several control variables which have been documented in the previous literature. The control variables are: the term spread (TERM), which measures the difference between the 10-year Treasury bond rate and the three-month Treasury bill rate; the default spread (DEF), which is the difference between the yields of the Moody's AAA and BAA corporate bonds; the TED spread, which represents the difference between the three-month U.S. Libor rate and the three-month Treasury bill rate; the Fama–French high minus low (HML); small minus big (SMB); momentum (MOM); and the Baltic Dry Index (BDI). The monthly values

[11]CFNAI is a weighted average of 85 existing monthly national economic activity indicators. The 85 economic indicators considered in CFNAI contain information from four broad categories: (1) production and income, (2) employment, unemployment, and hours, (3) personal consumption and housing, (4) sales, orders, and inventories. Since economic activity tends toward trend growth rate over time, a positive/negative CFNAI value corresponds to growth above/below trend. The six economic indicators considered in ADS are: weekly initial jobless claims, monthly payroll employment, industrial production, personal income less transfer payments, manufacturing and trade sales, and quarterly real GDP. A positive/negative ADS value suggests a better-than-average/worse-than-average economic condition. CFNAI and ADS reflect growth or recession by construction, so it is unnecessary to compute the growth rates for these two REA proxies.

Table 3: Summary Statistics and Correlation Matrix of the Real Economic Activity Proxies

	IP	NFP	RS	HS	CFNAI	ADS
Panel A. Summary Statistics						
Mean	0.0005	0.0004	0.0013	-0.0008	-0.1410	-0.3890
Std	0.0119	0.0097	0.0181	0.0831	1.3300	2.1305
Min	-0.1356	-0.1480	-0.1511	-0.3065	-17.7400	-24.6831
Max	0.0585	0.0353	0.1684	0.2148	5.8700	8.1819
Skew	-5.7235	-13.4045	0.7541	-0.1907	-8.6262	-7.4901
Kurt	71.7208	208.6089	50.8315	3.3107	121.1685	83.9796
Panel B. Correlation Matrix						
IP	1.0000					
NFP	0.8175	1.0000				
RS	0.5863	0.6600	1.0000			
HS	0.3446	0.2906	0.3435	1.0000		
CFNAI	0.9229	0.9363	0.7419	0.3884	1.0000	
ADS	0.8766	0.8201	0.6140	0.3479	0.8935	1.0000

Note: This table presents the summary statistics (in Panel A) and the correlation matrix (in Panel B) for the real economic activity proxies. The selected proxies are: IP, the logarithmic growth rate of industrial production, NFP, the logarithmic growth rate of nonfarm payroll employment, RS, the logarithmic growth rate of retail sale, HS, the logarithmic growth rate of housing starts, CFNAI, the Chicago Fed National Activity Index, and ADS, the Aruoba–Diebold–Scotti (Aruoba et al., 2009) business conditions index. The sample period is from January 1999 to October 2020.

of these control variables are obtained from January 1999 to October 2020. The data on TERM, DEF and TED is obtained from the FRED. The Fama-French factors are downloaded from Kenneth French's website and the BDI historical series is collected from Bloomberg.

Our goal is to predict the REA growth, and we expect that the change in FERP is an appropriate predictive factor. We analyze the relationship between FERP and the REA growth, with the results reported in the Supplementary Appendix. We find that the once-lagged and twice-lagged FERP have similar (but with opposing signs) effects on the future REA growth, which suggests that it is actually the change in the FERP that has a predictive impact on REA growth.

We regress each one of the REA growth proxies over forecasting horizons of length h on the change in FERP, which is defined as $\Delta FERP_t = FERP_t - FERP_{t-1}$, by using the earlier described set of control variables:

$$REA_{t+h} = \alpha + \beta_1 \Delta FERP_t + \beta_2 REA_t + \beta_c^{'} Control_t + \epsilon_{t+h}. \tag{7}$$

where REA_{t+h} denotes the growth in the REA proxies over the period from t to $t+h$, and REA_t

denotes the growth in the REA proxies from $t-h$ to t. We set $h = 1, 2, 4, 6$ months for the predictive regression setting as in Faccini et al. (2019).

Table 4: Forecasting Real Economic Activity Proxies using the Change in Forward Equity Risk Premium—In-Sample and Out-of-Sample Results

	SV			SVJ			NGARCH		
	Coef	Adj. R^2	OSR^2	Coef	Adj. R^2	OSR^2	Coef	Adj. R^2	OSR^2
Panel A. h =1M									
IP	-0.17***	0.25	0.08	-0.15***	0.24	0.07	0.04***	0.19	-0.11
NFP	-0.15***	0.22	0.13	-0.14***	0.21	0.11	0.03**	0.15	0.05
RS	-0.35***	0.18	0.15	-0.30***	0.15	0.12	0.01	0.03	-0.01
HS	-0.60***	0.21	0.02	-0.59***	0.21	0.02	0.16	0.20	-0.02
CFNAI	-23.77***	0.26	0.14	-21.93***	0.24	0.12	5.19***	0.16	0.01
ADS	-29.43***	0.46	0.06	-24.39***	0.44	0.04	4.76**	0.39	-0.02
Panel B. h =2M									
IP	-0.26***	0.17	-0.56	-0.23***	0.16	-0.60	0.05**	0.11	-1.03
NFP	-0.24***	0.18	0.04	-0.21***	0.17	0.03	0.05**	0.14	-0.01
RS	-0.30***	0.11	-0.02	-0.21***	0.09	-0.01	-0.01	0.06	-0.14
HS	-1.33***	0.26	0.03	-1.17***	0.25	0.03	-0.14	0.19	-0.09
CFNAI	-31.46***	0.17	0.06	-26.21***	0.15	0.06	5.57*	0.09	-0.03
ADS	-48.91***	0.21	0.07	-39.03***	0.19	0.04	7.44	0.15	-0.04
Panel C. h =4M									
IP	-0.24***	0.15	-1.08	-0.19**	0.14	-1.04	0.06*	0.13	-1.29
NFP	-0.19**	0.19	0.01	-0.15**	0.19	0.02	0.05	0.18	0.00
RS	-0.21**	0.15	0.01	-0.19**	0.14	0.01	0.01	0.13	0.00
HS	-0.63*	0.24	0.02	-0.58*	0.24	0.02	0.14	0.23	-0.15
CFNAI	-28.06***	0.18	0.03	-22.98***	0.17	0.03	6.62*	0.15	-0.09
ADS	-51.71***	0.09	0.00	-40.19**	0.08	0.01	10.62	0.07	-0.01
Panel D. h =6M									
IP	-0.07	0.24	-1.04	-0.06	0.24	-1.00	0.01	0.24	-1.51
NFP	-0.08	0.21	0.01	-0.08	0.21	0.02	0.05	0.21	0.00
RS	0.07	0.19	-0.01	0.02	0.19	0.00	-0.01	0.19	-0.02
HS	-0.39	0.25	0.03	-0.43	0.25	0.02	-0.20	0.25	-0.53
CFNAI	-6.11	0.35	0.01	-4.48	0.35	0.03	-0.87	0.35	-0.04
ADS	-3.62	0.16	0.00	-2.23	0.16	0.02	4.40	0.16	0.01

Note: This table reports the results based on equation (7). The dependent variable is one of the six selected proxies for real economic activities over an h-month horizon ($h = 1, 2, 4, 6$). The estimated coefficients and adjusted R^2 (Adj. R^2) are reported. *, ** and *** indicate values significant at 10%, 5% and 1% significance levels, respectively. We also report the out-of-sample R^2 (OSR^2) comparing Equation (7) with the benchmark model that considers only the lagged REA and the control variables as predictors. We consider the data period from January 1999 to December 2003 as the in-sample estimation period and January 2004 to October 2020 as the out-of-sample performance evaluation period. We run the regressions each month after January 2004 recursively with expanding windows using historical data from January 1999.

Besides the in-sample prediction of the U.S. REA growth, we also assess the predictive ability of the change in FERP in a real-time out-of-sample setting over January 2004 to October 2020. We consider the data period from January 1999 to December 2003 as the in-sample estimation period. For each REA growth proxy, we run the predictive regression (7) recursively from January

2004 by adding new observations and re-estimating the regression. We compare Equation (7) with the benchmark model that considers only the lagged REA and the control variables as predictors. Following Faccini et al. (2019), we compute the out-of-sample R^2 (OSR^2) using the method of Campbell and Thompson (2008), which shows the outperformance of the model by computing the percentage of the variation not explained by the benchmark model that has captured by the full model:

$$\text{OS}R^2 = 1 - \frac{\text{var}\left[\text{E}_t(REA_{t+h}^{Full}) - REA_{t+h}\right]}{\text{var}\left[\text{E}_t(REA_{t+h}^{Benchmark}) - REA_{t+h}\right]}, \tag{8}$$

where $\text{E}_t(REA_{t+h}^{Full})$ and $\text{E}_t(REA_{t+h}^{Benchmark})$ denote the h-month ahead forecast from the full and benchmark model, respectively. The forecasts $\text{E}_t(REA_{t+h}^{Full})$ from the full model are:

$$\text{E}_t(REA_{t+h}^{Full}) = \widehat{\alpha} + \widehat{\beta}_1 \Delta FERP_t + \widehat{\beta}_2 REA_t + \widehat{\beta}_c' Control_t, \tag{9}$$

and the forecasts $\text{E}_t(REA_{t+h}^{Benchmark})$ from the benchmark model are given by:

$$\text{E}_t(REA_{t+h}^{Benchmark}) = \widehat{\alpha_b} + \widehat{\beta_{2,b}} REA_t + \widehat{\beta_{c,b}'} Control_t, \tag{10}$$

where $\widehat{\alpha}$, $\widehat{\beta}_1$, $\widehat{\beta}_2$ and $\widehat{\beta}_c'$ in (9) are the estimated regression coefficients of the full model, and $\widehat{\alpha_b}$, $\widehat{\beta_{2,b}}$ and $\widehat{\beta_{c,b}'}$ in (10) are the estimated regression coefficients of the benchmark model. A positive/negative out-of-sample R^2 indicates that the full model outperforms/underperforms the benchmark model. The change in FERP has out-of-sample predictive ability if the out-of-sample R^2 is positive.

Table 4 presents both the in-sample estimated coefficients and adjusted R^2 as well as the out-of-sample R^2. The estimated coefficients of $\Delta FERP$ implied by SV and SVJ are all significantly negative for short and intermediate forecasting horizons ($h = 1, 2, 4$ months), indicating that the

REA growth decreases with the change in FERP estimated by SV and SVJ. This result is consistent with Faccini et al. (2019) as the FERP is positively linked to investors' risk aversion when the forward-looking physical skewness of the returns is negative and the kurtosis is greater than 3 by construction as demonstrated in Equation (3). Our approach is different from Faccini et al. (2019) in two aspects: (1) the subject of our study is FEPR, which is constructed with the risk aversion coefficient; (2) the risk aversion coefficient in our study is estimated with the physical moments of the returns and the implied volatility, while Faccini et al. (2019) use option implied higher-order moments and realized volatility. The out-of-sample results for the FERP obtained from the SV model are marginally better than the ones obtained using the SVJ model. Both models produce better out-of-sample R^2 values than the ones obtained using the FERP values based on the NGARCH model. The effect of the one-month FERP on REA growth fades with the forecasting horizon as we observe no significant coefficients when $h = 6$.

Furthermore, the one-month FERP estimated by SV and SVJ reveal positive out-of-sample R^2 at the one-month forecasting horizon for all REA proxies. In contrast, the out-of-sample R^2 for the NGARCH FERP is negative in most cases, implying a weak predictive power of the NGARCH FERP for most of the REA growth indicators.

Using the FERP obtained by the SV, SVJ and NGARCH models, Equation (9) can lead to three sets of forecasts. In order to examine the REA growth forecasting performance of the FERP implied by the different models, we perform the Diebold and Mariano (2002) (DM) tests for forecasting errors. The null hypothesis of the DM test is that the forecasting errors, which are defined as $\mathrm{E}_t(REA_{t+h}^{Full}) - REA_{t+h}$, of the two competing models, are equal. Table 5 reports the DM statistics, and rejections of the null hypothesis are denoted using stars. Consistent with previous findings, the SV and SVJ FERPs generally lead to significantly lower forecasting errors than the NGARCH FERP, for almost all the REA growth proxies and forecasting horizons considered. Additionally,

most of the forecasting errors obtained by the SV and SVJ FERP reveal no significant differences.

Table 5: DM Statistics for the Real Economic Activity Growth Forecasting Errors

	1M		2M		4M		6M	
				IP				
	SVJ	NGARCH	SVJ	NGARCH	SVJ	NGARCH	SVJ	NGARCH
SV	-1.09	-1.41*	-1.47*	-1.51*	-1.84**	-1.39*	-1.09	-1.52*
SVJ		-1.36*		-1.42*		-1.23		-1.49*
				NFP				
	SVJ	NGARCH	SVJ	NGARCH	SVJ	NGARCH	SVJ	NGARCH
SV	-1.02	-1.03	-0.66	-1.03	-0.85	-1.08	-1.13	-0.98
SVJ		-1.03		-1.24		-1.11		-0.98
				RS				
	SVJ	NGARCH	SVJ	NGARCH	SVJ	NGARCH	SVJ	NGARCH
SV	-1.25	-1.40*	0.15	-0.91	-0.50	-0.45	2.09**	-1.31*
SVJ		-1.42*		-0.94		-0.42		-1.87**
				HS				
	SVJ	NGARCH	SVJ	NGARCH	SVJ	NGARCH	SVJ	NGARCH
SV	-0.47	-1.36*	-0.43	-1.55*	-0.36	-1.50*	-0.07	-1.46*
SVJ		-1.37*		-1.43*		-1.47*		-1.45*
				CFNAI				
	SVJ	NGARCH	SVJ	NGARCH	SVJ	NGARCH	SVJ	NGARCH
SV	-1.15	-1.13	-0.70	-1.58*	-0.78	-1.74**	-1.40*	-1.27*
SVJ		-1.13		-1.72**		-1.71**		-1.24
				ADS				
	SVJ	NGARCH	SVJ	NGARCH	SVJ	NGARCH	SVJ	NGARCH
SV	-0.98	-1.11	-0.97	-1.03	-0.29	-0.32	0.20	1.30*
SVJ		-1.16		-1.06		-0.30		1.29*

Notes: This table reports DM statistics for out-of-sample REA growth forecasting errors using the FERP obtained with the SV, SVJ and NGARCH models. The out-of-sample performance evaluation period ranges from January 2004 to October 2020. We consider six REA growth proxies and four forecasting horizons (1, 2, 4 and 6 months). * and ** indicate values significant at 10% and 5% significance levels for the one-sided test, respectively. A negative (positive) value indicates that the row model has smaller (larger) forecasting errors than the corresponding column model.

Overall, the change in the one-month FERP estimated by SV and SVJ has good predictive power for all REA growth proxies, especially at the one-month forecasting horizon, performing better than the FERP estimated using the NGARCH model. The predictive ability of the one-month ahead FERP fades with the forecasting horizon, disappearing at the six-month horizon. Consistent with economic intuition, we find that an increase in the FERP, estimated using the SV and SVJ models, leads to a decrease in REA growth, whilst the effect is reversed for the NGARCH model.

6 Forecasting Market Excess Returns using Quantile Regressions

The equity risk premium is expected to be related to the excess returns of assets, and here we test whether it is able to forecast the realized cumulative excess returns. Duan and Zhang (2014), using linear regressions, find that the quarterly market excess return is negatively linked to the FERP. This suggests that taking on risk leads to losses which makes sense during market crashes. However, this negative effect should not always hold as it conflicts with the risk-return tradeoff. Whitelaw (2000) proposes an equilibrium model implying that the relationship between market risk and returns should be non-linear. Furthermore, the predictability of market returns should be stronger under good market conditions as unsophisticated investors tend to enter the stock market following good times (Lemmon and Portniaguina, 2006; Grinblatt and Keloharju, 2009). Other studies find that the predictability of market returns improves during recessions (Garcia, 2013; Cujean and Hasler, 2017).

In this section, we discuss the role of FERP in predicting market excess returns using quantile regressions. Quantile regressions are an appropriate tool to identify the more complex association spectrum between the FERP and the future cumulative market excess returns; specifically, they can differentiate between bull and bear market conditions. The varying market conditions are captured by different quantiles of the conditional distribution; upper/lower quantiles are associated with good/bad states (Li et al., 2015). Furthermore, in the following we also test for non-linear relationships between the variables investigated.

We regress the realized cumulative market excess return over h forecasting horizons on FERP. The conditional quantile function of the market excess returns at quantile $\varpi \in (0, 1)$ given the regressor FERP is:

$$Q_{\varpi}(R_{M,t+h} - r_{t+h}|FERP_t) = \alpha_{\varpi} + \beta_{\varpi} FERP_t + \epsilon_{\varpi,t+h}, \tag{11}$$

Table 6: Forecasting Market Excess Returns—Quantile Regression Results

		0.1	0.2	0.3	0.4	0.5	0.6	0.7	0.8	0.9
Panel A. h =1M										
SV	Coef	-0.52***	-0.18*	-0.20**	-0.13	-0.04	0.15*	0.28***	0.47***	0.60***
	pR^2(%)	5.33	1.42	1.35	0.5	0.12	0.27	2.45	6.98	15.27
SVJ	Coef	-0.54***	-0.18*	-0.25***	-0.16*	-0.05	0.06	0.26***	0.42***	0.49***
	pR^2(%)	4.88	1.47	1.42	0.65	0.16	0.1	2.19	5.95	13.34
NGARCH	Coef	-0.43***	-0.51***	-0.19***	-0.13***	-0.14***	-0.02	-0.03	0.28***	0.50***
	pR^2(%)	4.7	3.39	1.64	1.25	0.63	0.18	0.07	1.53	4.78
Panel B. h =2M										
SV	Coef	-0.18	-0.35**	-0.25*	-0.03	-0.06	0.11	0.3**	0.41***	0.83***
	pR^2(%)	0.91	1.07	0.34	0.01	0.01	0.2	1.85	4.65	10.4
SVJ	Coef	-0.21	-0.39***	-0.32**	-0.03	-0.07	0.1	0.25**	0.27**	0.83***
	pR^2(%)	1.23	1.84	0.97	0.07	0.12	0.15	1.59	3.46	7.08
NGARCH	Coef	-0.73***	-0.09	-0.14	-0.12	-0.14*	-0.16**	-0.18***	0.41***	0.61***
	pR^2(%)	1.39	1.53	1.7	1.33	1.25	0.78	0.3	1.07	4.98
Panel C. h =6M										
SV	Coef	-0.77***	-0.79***	-0.7***	-0.15	-0.1	0.06	0.22	1.04***	1.27***
	pR^2(%)	1.65	2.46	0.98	0.1	0.23	0.03	0.26	2.56	11.53
SVJ	Coef	-0.93***	-0.68***	-0.75***	-0.28	-0.14	-0.09	0.07	0.49***	1.27***
	pR^2(%)	1.75	2.81	1.84	0.43	0.49	0.05	0.07	1.18	9.01
NGARCH	Coef	0	-0.1	-0.16	-0.21	-0.05	-0.06	0.05	0.51***	1.2***
	pR^2(%)	0.02	0.63	0.54	0.17	0.2	0.13	0.05	1.68	6.17
Panel D. h =12M										
SV	Coef	-1.49**	-2.13***	-1.56***	-0.85***	-0.08	-0.1	0.13	0.64***	1.18***
	pR^2(%)	2.2	6.73	3.71	0.34	0.07	0.04	0.15	1.61	5.49
SVJ	Coef	-2.08***	-2.42***	-1.56***	-0.68**	-0.17	-0.22	0.1	0.48**	0.93***
	pR^2(%)	3.44	8.16	4.79	1.2	0.26	0.16	0.04	1.04	3.39
NGARCH	Coef	0.43	0.21	0.07	0.02	0.22	0.18	0.63***	0.71***	0.7***
	pR^2(%)	0.32	0.04	0.13	0.06	0.29	0.67	1.26	3.3	5.19

Note: This table reports the results of the quantile regression (11) based on equally spaced quantiles from 0.1 to 0.9 for an h-month forecasting horizon ($h = 1, 2, 6, 12$). The sample period is from January 1999 to October 2020. The estimated coefficients and pseudo R^2 (pR^2) in percentage are reported. *, ** and *** indicate values significant at 10%, 5% and 1% significance levels, respectively.

where $R_{M,t+h}$ denotes the return on the S&P 500 index over the period t to $t+h$ and r_{t+h} is the risk-free rate over the period t to $t+h$. The risk-free rate is obtained from the U.S. Department of the Treasury website.

Table 6 reports the results of the quantile regressions for various forecasting horizons ($h = 1, 2, 6, 12$). The best predictive power for FERP is revealed for the one-month horizon for all quantiles. To present the results visually, we also plot the quantile regression coefficients and pseudo R^2 in Figure 6 for the one-month horizon. According to these results, the FERP estimated by all

Figure 6: Quantile Regression Results

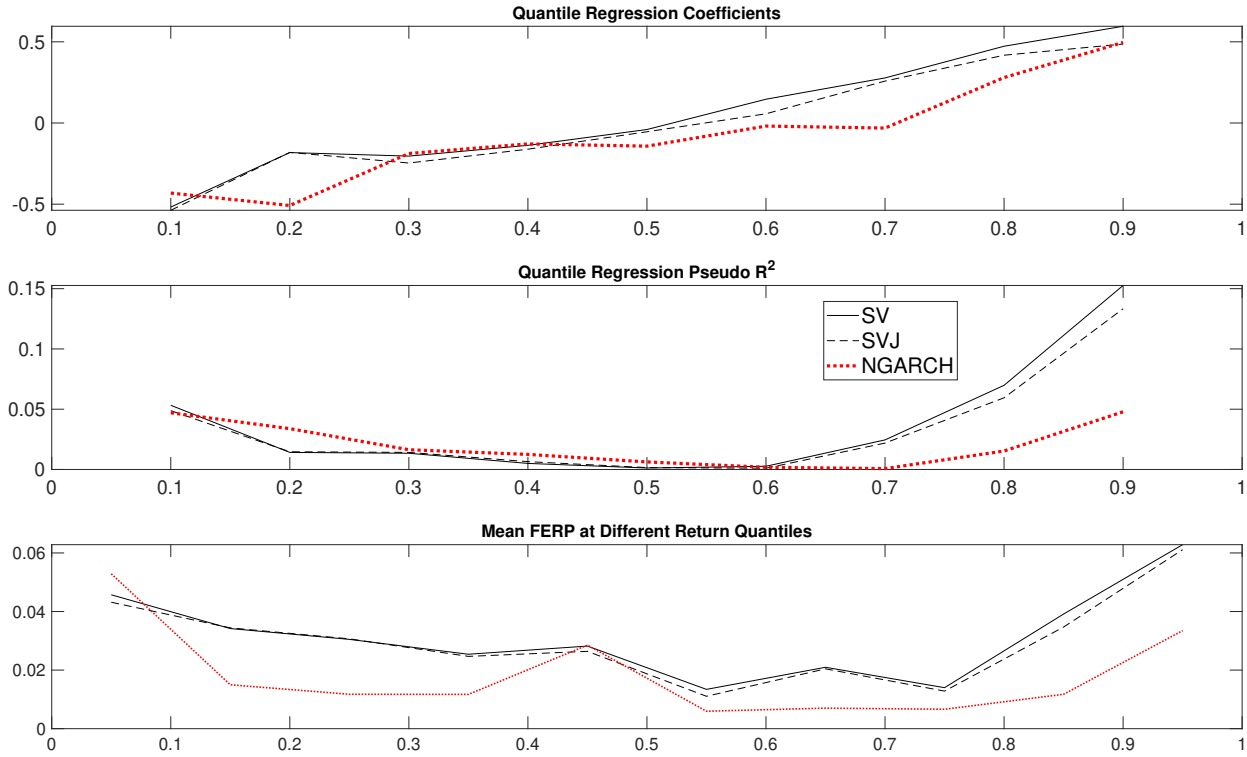

Note: This figure presents the results of the quantile regression (11) for equally spaced quantiles from 0.1 to 0.9 for the one-month forecasting horizon ($h = 1$). The sample period is from January 1999 to October 2020. The estimated coefficients and pseudo R^2 are plotted in the top and middle panels, respectively. The bottom panel plots the average FERP values when the realized one-month market excess return lies in different quantiles (e.g., 0-quantile to 0.1-quantile, 0.1-quantile to 0.2-quantile,..., 0.9-quantile to 1-quantile.).

models has forecasting power for the future market excess returns for seven out of nine quantiles. Compared with the NGARCH FERP, the SV and SVJ FERPs have a stronger predictive power in the upper quantiles (0.7, 0.8 and 0.9) and in the 0.1 quantile. However, the NGARCH FERP series has the highest pseudo R^2 for the quantiles 0.2 to 0.5. The FERP estimated with SV is found to have a slightly better predictive ability than the one estimated by SVJ.[12] The coefficient values increase with the quantiles, from just over -0.6 at the 0.1 quantile to around 0.6 at the

[12]The FERP obtained through the SVJ model has somewhat worse performance in predicting REA growth and market excess returns compared with the SV FERP. A possible explanation is that the jump parameters are notoriously difficult to estimate as jumps are very rare events (these difficulties are well documented in Broadie et al., 2007; Li et al., 2008 and Christoffersen et al., 2012); the low probability of jump occurrence, together with the poor estimates of jump parameters, make it difficult to get good estimates for the SVJ FERP.

0.9 quantile, implying a differentiation of the effect of FERP on excess returns, according to the quantiles. The estimated coefficients are significantly negative for the lower quantiles and positive at upper quantiles, indicating that the realized cumulative market excess returns decrease with the FERP in a bear market and increase with FERP in a bull market. These results also partially accommodate the results of Duan and Zhang (2014), e.g., the NGARCH FERP is significantly negatively linked to the future cumulative returns at the 0.5 quantile. Based on the bottom panel of Figure 6, the lagged FERP also tends to be high in the extreme tails.

The one-month ahead FERPs estimated by SV and SVJ have a significant effect on the lower tails of the future cumulative market excess returns for short, intermediate and long forecasting horizons ($h = 1, 2, 6, 12$), while the NGARCH FERP reveals no significant impact on the left tails of the realized cumulative market excess returns for longer forecasting horizons ($h = 6, 12$). Interestingly, the pseudo R^2 reaches its largest values for the 0.9 quantile for all forecasting horizons. This is consistent with Lemmon and Portniaguina (2006) and Grinblatt and Keloharju (2009), who conclude that unsophisticated investors are more likely to enter the stock market following good times rather than bad times, and therefore the predictability is higher in a bullish market. Overall, the forecasting ability of FERP is the highest for the extreme quantiles.

Our findings show that the FERP contains significant information about the extreme tails of the future cumulative market excess returns. The forecasting ability is the strongest for the upper quantiles. The FERP is positively (negatively) related to the future market excess returns when the market is bullish (bearish), suggesting that investors require a forward premium to hold the market asset during bull markets, being exposed to possible bearish market downturns.

7 Conclusions

We estimate the one-month forward-looking market risk premium of the S&P 500 index based on the framework proposed by Duan and Zhang (2014) but using stochastic volatility models. The forward-looking physical moments of the returns are deduced using a simulation method for three models, namely the SV, SVJ and the NGARCH models. Considering the estimated return residuals, we find that the SV and SVJ models fit the data better than the NGARCH model. The FERP estimated by all models is high and positive during the turbulent periods before 2020. However, only the FERPs estimated by SV and SVJ respond to the COVID-19 pandemic in 2020 with a sudden positive spike, while the NGARCH FERP is negative during the same period. Furthermore, only the FERP implied by the SV model stays positive for the entire research period.

We also study the economic implications of FERP from two aspects: the prediction of (1) real economic activities and of (2) cumulative market excess returns using FERP. We observe a better predictive ability of the FERPs estimated under the SV and SVJ models.

Our analysis shows that the changes in the FERP estimated using the SV and SVJ models have a negative effect on the U.S. REA growth. Additionally, the FERP contains predictive information about the extreme tails of the future cumulative market excess returns. We show that the cumulative excess returns increase with the FERP in bull markets and decrease with FERP when the market is bearish.

Appendix A Priors for Model Parameters

The priors in the paper are consistent with the literature (Eraker et al., 2003) and are summarized here: $\mu \sim \mathbb{N}(0, 100)$, $\kappa \sim \mathbb{N}(0, 1)\mathbf{1}_{\kappa>0}$, $\theta \sim \mathbb{N}(0, 1)\mathbf{1}_{\theta>0}$, $\rho \sim \mathbb{U}(-1, 1)$, $\sigma_v^2 \sim \mathbb{IG}(2.5, 0.1)$, $\mu_J \sim \mathbb{N}(0, 100)$, $\sigma_J^2 \sim \mathbb{IG}(10, 40)$ and $\lambda \sim \mathbb{B}(2, 40)$. $\mathbb{IG}$ refers to the Inverse Gamma distribution, $\mathbb{U}$

represents the standard Uniform distribution, and $\mathbb{B}$ stands for the Beta distribution.

Appendix B MCMC Estimation Methods

Posterior distributions and updating algorithms for parameters and latent variables are detailed in this section. Δ denotes the time interval. We introduce posteriors for the SVJ model below. The SVJ model becomes SV by setting $\lambda = 0$.

Posterior for μ: $\mu|Y, V, J^Y, \Theta\backslash\{\mu\} \sim \mathbb{N}(\mathcal{A}, \mathcal{B})$, where $\mathcal{B} = \mathcal{A}\frac{\Delta}{(1-\rho^2)}\sum_{t=0}^{T-1}\frac{H_{t+1}-\frac{\rho}{\sigma_v}D_{t+1}}{V_t} + \frac{c^*}{C^*}$, $\mathcal{A} = \left[\frac{\Delta^2}{(1-\rho^2)}\sum_{t=0}^{T-1}\frac{1}{V_t} + \frac{1}{C^*}\right]^{-1}$, $D_{t+1} = V_{t+1} - V_t - \kappa(\theta - V_t)\Delta$, and $H_{t+1} = Y_{t+1} - Y_t - J^Y_{t+1}$. $c^* = 0$ and $C^* = 100$ are hyperparameters of the prior of μ.

Posterior for κ: $\kappa|Y, V, J^Y, \Theta\backslash\{\kappa\} \sim \mathbb{N}\left(\frac{\mathcal{A}}{\mathcal{B}}, \sqrt{\frac{1}{\mathcal{B}}}\right)\mathbf{1}_{\kappa>0}$, where $\mathcal{B} = \frac{\Delta}{(1-\rho^2)\sigma_v^2}\sum_{t=0}^{T-1}\frac{(\theta-V_t)^2}{V_t} + 1$, $\mathcal{A} = \frac{1}{\sigma_v(1-\rho^2)}\sum_{t=0}^{T-1}\frac{(\theta-V_t)\frac{V_{t+1}-V_t}{\sigma_v} - \rho H_{t+1}}{V_t}$, and $H_{t+1} = Y_{t+1} - Y_t - \mu\Delta - J^Y_{t+1}$.

Posterior for θ: $\theta|Y, V, J^Y, J^V, \Theta\backslash\{\theta\} \sim \mathbb{N}\left(\frac{\mathcal{A}}{\mathcal{B}}, \sqrt{\frac{1}{\mathcal{B}}}\right)\mathbf{1}_{\theta>0}$, where $\mathcal{B} = \frac{\kappa^2\Delta}{(1-\rho^2)\sigma_v^2}\sum_{t=0}^{T-1}\frac{1}{V_t} + 1$, $\mathcal{A} = \frac{\kappa}{\sigma_v(1-\rho^2)}\sum_{t=0}^{T-1}\frac{\frac{D_{t+1}}{\sigma_v} - \rho H_{t+1}}{V_t}$, $D_{t+1} = V_{t+1} + (\kappa\Delta - 1)V_t$, and $H_{t+1} = Y_{t+1} - Y_t - \mu\Delta - J^Y_{t+1}$.

Posterior for $\sigma_v^2 \propto (\sigma_v^2)^{\frac{T+c^*+2}{2}} \times \pi(\sigma_v) \times \exp\left\{-\frac{1}{2}\frac{C^*}{\sigma_v^2}\right\}$, where $c^* = 2.5$, and $C^* = 0.1$ are hyperparameters of the prior of σ_v^2, and $\pi(\sigma_v) := \exp\left\{-\frac{1}{2}\sum_{t=0}^{T-1}\frac{(D_{t+1}-\rho\sigma_v(H_{t+1}))^2}{(1-\rho^2)\sigma_v^2 V_t\Delta}\right\}$. $D_{t+1} = V_{t+1} - V_t - \kappa(\theta - V_t)\Delta$ and $H_{t+1} = Y_{t+1} - Y_t - \mu\Delta - J^Y_{t+1}$. The updating algorithm is: (1) for a given previous draw $\sigma_v^{(g)}$, draw $\sigma_v^{(g+1)}$ from the proposal density function $\mathbb{IG}(\mathcal{A}, \mathcal{B})$, where $\mathcal{A} = c^* + T$ and $\mathcal{B} = C^* + \sum_{t=0}^{T-1}\frac{D_{t+1}^2}{V_t\Delta}$, (2) accept $\sigma_v^{(g+1)}$ with probability $\min\left(\frac{\pi(\sigma_v^{(g+1)})}{\pi(\sigma_v^{(g)})}, 1\right)$.

Posterior for $\rho \propto \pi(\rho) := (1-\rho^2)^{-\frac{T}{2}}\exp\{-12(1-\rho^2)\sum_{t=0}^{T-1}(H_{t+1}^2 + D_{t+1}^2) + \frac{\rho}{1-\rho^2}\sum_{t=0}^{T-1} H_{t+1}D_{t+1}\}$, where $D_{t+1} = \frac{V_{t+1}-V_t-\kappa(\theta-V_t)\Delta}{\sigma_v\sqrt{V_t\Delta}}$ and $H_{t+1} = \frac{Y_{t+1}-Y_t-\mu\Delta-J^Y_{t+1}}{\sqrt{V_t\Delta}}$. The estimation is updated using the following algorithm: (1) Draw $\frac{1}{2}\ln\frac{1+\rho^{(g+1)}}{1-\rho^{(g+1)}}$ from $\mathbb{N}\left(\frac{1}{2}\ln\frac{1+\rho_r}{1-\rho_r}, \frac{1}{T-3}\right)$, where $\rho_r = Corr(\mathbf{D}, \mathbf{H})$, $\mathbf{D} = \{D_{t+1}\}_{t=0}^{T-1}$, $\mathbf{H} = \{H_{t+1}\}_{t=0}^{T-1}$, and $Corr$ denotes correlation; (2) accept ρ^{g+1} with $\min\left(\frac{\pi\left(\rho^{(g+1)}\right)}{\pi\left(\rho^{(g)}\right)} \times \frac{\exp\left(-\frac{\left(f\left(\rho^{(g)}\right)-f(\rho_r)\right)^2}{\frac{2}{T-3}}\right)}{\exp\left(-\frac{\left(f\left(\rho^{(g+1)}\right)-f(\rho_r)\right)^2}{\frac{2}{T-3}}\right)}, 1\right)$, where $f(\rho) = \frac{1}{2}\ln\frac{1+\rho}{1-\rho}$.

Posterior for μ_J: $\mu_J|\xi^Y,\xi^V,\Theta\backslash\{\mu_J\} \sim \mathbb{N}\left(\frac{\mathcal{A}}{\mathcal{B}},\sqrt{\frac{1}{\mathcal{B}}}\right)$, where $\mathcal{A}=\sum_{t=0}^{T-1}\frac{\left(\xi^Y_{t+1}\right)}{\sigma_J^2}+\frac{c^*}{C^*}$, $\mathcal{B}=\frac{T}{\sigma_J^2}+\frac{1}{C^*}$, $c^*=0$ and $C^*=100$ are hyperparameters of the prior of μ_J.

Posterior for σ_J^2: $\sigma_J^2|\xi^Y,\xi^V,\Theta\backslash\{\sigma_J\} \sim \mathbb{IG}(\mathcal{A},\mathcal{B})$, where $\mathcal{A}=c^*+T$, $\mathcal{B}=C^*+\sum_{t=0}^{T-1}(\xi^Y_{t+1}-\mu_J)^2$, $c^*=10$ and $C^*=40$ are hyperparameters of the prior of σ_J^2.

Posterior for λ: $\lambda|N \sim \mathbb{B}(\mathcal{A},\mathcal{B})$, where $\mathcal{A}=c^*+\sum_{t=0}^{T-1}N_{t+1}$, $\mathcal{B}=C^*+T-\sum_{t=0}^{T-1}N_{t+1}$, $c^*=2$ and $C^*=40$ are hyperparameters of the prior of λ.

Posterior for N: $N_{t+1}|Y,V,\xi^Y,\xi^V,\Theta \sim Bernoulli\left(\frac{\alpha_1}{\alpha_1+\alpha_2}\right)$. *Bernoulli* denotes the Bernoulli distribution. $\alpha_1=\lambda\exp\left(-\frac{1}{2(1-\rho^2)}\left(H_{t+1}^2-2\rho H_{t+1}D_{t+1}\right)\right)$, $D_{t+1}=\frac{V_{t+1}-V_t-\kappa(\theta-V_t)\Delta}{\sigma_v\sqrt{V_t\Delta}}$, $H_{t+1}=\frac{Y_{t+1}-Y_t-\mu\Delta-\xi^Y_{t+1}}{\sqrt{V_t\Delta}}$, $HH_{t+1}=\frac{Y_{t+1}-Y_t-\mu\Delta}{\sqrt{V_t\Delta}}$, $\alpha_2=(1-\lambda)\exp\left(-\frac{1}{2(1-\rho^2)}\left(HH_{t+1}^2-2\rho HH_{t+1}DD_{t+1}\right)\right)$, and $DD_{t+1}=\frac{V_{t+1}-V_t-\kappa(\theta-V_t)\Delta}{\sigma_v\sqrt{V_t\Delta}}$.

Posterior for ξ^Y: $\xi^Y_{t+1}|Y,V,\xi^V,N_{t+1}=1,\Theta \sim \mathbb{N}\left(\frac{\mathcal{A}}{\mathcal{B}},\sqrt{\frac{1}{\mathcal{B}}}\right)$, where $\mathcal{A}=\frac{H_{t+1}-\frac{\rho}{\sigma_v}D_{t+1}}{(1-\rho^2)V_t\Delta}+\frac{\mu_J}{\sigma_J^2}$, $\mathcal{B}=\frac{1}{(1-\rho^2)V_t\Delta}+\frac{1}{\sigma_J^2}$, $D_{t+1}=V_{t+1}-V_t-\kappa(\theta-V_t)\Delta$, and $H_{t+1}=Y_{t+1}-Y_t-\mu\Delta$.

Posterior for $V \propto \pi(V_{t+1}) := \frac{1}{V_{t+1}}\times\exp\left\{-\frac{-2\rho D_{t+1}H_{t+1}+D_{t+1}^2}{2(1-\rho^2)}-\frac{D_{t+2}^2-2\rho D_{t+2}H_{t+2}+H_{t+2}^2}{2(1-\rho^2)}\right)$, for $0<t+1<T$. $D_{t+1}=\frac{V_{t+1}-V_t-\kappa(\theta-V_t)\Delta}{\sigma_v\sqrt{V_t\Delta}}$, and $H_{t+1}=\frac{Y_{t+1}-Y_t-\mu\Delta-J^Y_{t+1}}{\sqrt{V_t\Delta}}$.

References

Abadie, A., 2002. Bootstrap tests for distributional treatment effects in instrumental variable models. Journal of the American Statistical Association 97, 284–292. doi:10.1198/016214502753479419.

Aït-Sahalia, Y., Lo, A.W., 2000. Nonparametric risk management and implied risk aversion. Journal of Econometrics 94, 9–51. doi:10.1016/S0304-4076(99)00016-0.

Amaya, D., Christoffersen, P., Jacobs, K., Vasquez, A., 2015. Does realized skewness predict the cross-section of equity returns? Journal of Financial Economics 118, 135–167. doi:10.1016/j.jfineco.2015.02.009.

Aruoba, S.B., Diebold, F.X., Scotti, C., 2009. Real-time measurement of business conditions. Journal of Business & Economic Statistics 27, 417–427. doi:10.1198/jbes.2009.07205.

Bae, J.W., Elkamhi, R., 2021. Global equity correlation in international markets. Management Science 67, 7262–7289. doi:10.1287/mnsc.2020.3780.

Bakshi, G., Madan, D., 2006. A theory of volatility spreads. Management Science 52, 1945–1956. doi:10.1287/mnsc.1060.0579.

Bali, T.G., Hovakimian, A., 2009. Volatility spreads and expected stock returns. Management Science 55, 1797–1812. doi:10.1287/mnsc.1090.1063.

Bekaert, G., Hoerova, M., 2014. The VIX, the variance premium and stock market volatility. Journal of Econometrics 183, 181–192. doi:10.1016/j.jeconom.2014.05.008.

Broadie, M., Chernov, M., Johannes, M., 2007. Model specification and risk premia: Evidence from futures options. Journal of Finance 62, 1453–1490. doi:10.1111/j.1540-6261.2007.01241.x.

Campbell, J.Y., Thompson, S.B., 2008. Predicting excess stock returns out of sample: Can anything beat the historical average? Review of Financial Studies 21, 1509–1531. doi:10.1093/rfs/hhm055.

Christoffersen, P., Jacobs, K., Ornthanalai, C., 2012. Dynamic jump intensities and risk premiums: Evidence from S&P500 returns and options. Journal of Financial Economics 106, 447–472. doi:10.1016/j.jfineco.2012.05.017.

Connolly, R., Stivers, C., Sun, L., 2005. Stock market uncertainty and the stock-bond return relation. Journal of Financial and Quantitative Analysis 40, 161–194. doi:10.1017/S0022109000001782.

Cujean, J., Hasler, M., 2017. Why does return predictability concentrate in bad times? Journal of Finance 72, 2717–2758. doi:10.1111/jofi.12544.

Diebold, F.X., Mariano, R.S., 2002. Comparing predictive accuracy. Journal of Business & Economic Statistics 20, 134–144. doi:10.1198/073500102753410444.

Doshi, H., Kumar, P., Yerramilli, V., 2018. Uncertainty, capital investment, and risk management. Management Science 64, 5769–5786. doi:10.1287/mnsc.2017.2815.

Drechsler, I., 2013. Uncertainty, time-varying fear, and asset prices. Journal of Finance 68, 1843–1889. doi:10.1111/jofi.12068.

Duan, J.C., Zhang, W., 2014. Forward-looking market risk premium. Management Science 60, 521–538. doi:10.1287/mnsc.2013.1758.

Engle, R.F., Ng, V.K., 1993. Measuring and testing the impact of news on volatility. Journal of Finance 48, 1749–1778. doi:10.1111/j.1540-6261.1993.tb05127.x.

Eraker, B., Johannes, M., Polson, N., 2003. The impact of jumps in volatility and returns. Journal of Finance 58, 1269–1300. doi:10.1111/1540-6261.00566.

Faccini, R., Konstantinidi, E., Skiadopoulos, G., Sarantopoulou-Chiourea, S., 2019. A new predictor of US real economic activity: The S&P 500 option implied risk aversion. Management Science 65, 4927–4949. doi:10.1287/mnsc.2018.3049.

Garcia, D., 2013. Sentiment during recessions. Journal of Finance 68, 1267–1300. doi:10.1111/jofi.12027.

Gourinchas, P.O., Obstfeld, M., 2012. Stories of the twentieth century for the twenty-first. American Economic Journal: Macroeconomics 4, 226–65. doi:10.1257/mac.4.1.226.

Grinblatt, M., Keloharju, M., 2009. Sensation seeking, overconfidence, and trading activity. Journal of Finance 64, 549–578. doi:10.1111/j.1540-6261.2009.01443.x.

Heston, S.L., 1993. A closed-form solution for options with stochastic volatility with applications to bond and currency options. Review of Financial Studies 6, 327–343. doi:10.1093/rfs/6.2.327.

Lemmon, M., Portniaguina, E., 2006. Consumer confidence and asset prices: Some empirical evidence. Review of Financial Studies 19, 1499–1529. doi:10.1093/rfs/hhj038.

Li, G., Li, Y., Tsai, C.L., 2015. Quantile correlations and quantile autoregressive modeling. Journal of the American Statistical Association 110, 246–261. doi:10.1080/01621459.2014.892007.

Li, H., Wells, M.T., Yu, C.L., 2008. A Bayesian analysis of return dynamics with Lévy jumps. Review of Financial Studies 21, 2345–2378. doi:10.1093/rfs/hhl036.

Maheu, J.M., McCurdy, T.H., Zhao, X., 2013. Do jumps contribute to the dynamics of the equity premium? Journal of Financial Economics 110, 457–477. doi:10.1016/j.jfineco.2013.07.006.

Rosenberg, J.V., Engle, R.F., 2002. Empirical pricing kernels. Journal of Financial Economics 64, 341–372. doi:10.1016/S0304-405X(02)00128-9.

Santa-Clara, P., Yan, S., 2010. Crashes, volatility, and the equity premium: Lessons from S&P 500 options. Review of Economics and Statistics 92, 435–451. doi:10.1162/rest.2010.11549.

Stock, J.H., Watson, M.W., 1999. Forecasting inflation. Journal of Monetary Economics 44, 293–335. doi:10.1016/S0304-3932(99)00027-6.

Stock, J.H., Watson, M.W., 2003. Forecasting output and inflation: The role of asset prices. Journal of Economic Literature 41, 788–829. doi:10.1257/002205103322436197.

Whitelaw, R.F., 2000. Stock market risk and return: An equilibrium approach. Review of Financial Studies 13, 521–547. doi:10.1093/rfs/13.3.521.

Yang, Z., Zhou, Y., 2017. Quantitative easing and volatility spillovers across countries and asset classes. Management Science 63, 333–354. doi:10.1287/mnsc.2015.2305.